Provided for non-commercial research and education use.
Not for reproduction, distribution or commercial use.

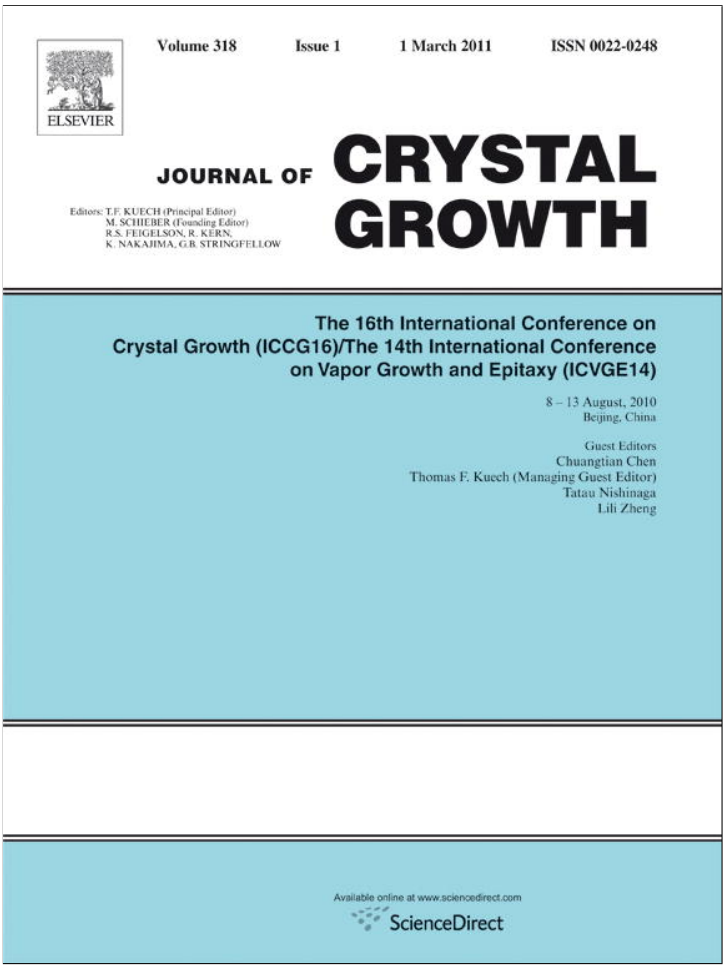

This article appeared in a journal published by Elsevier. The attached copy is furnished to the author for internal non-commercial research and education use, including for instruction at the authors institution and sharing with colleagues.

Other uses, including reproduction and distribution, or selling or licensing copies, or posting to personal, institutional or third party websites are prohibited.

In most cases authors are permitted to post their version of the article (e.g. in Word or Tex form) to their personal website or institutional repository. Authors requiring further information regarding Elsevier's archiving and manuscript policies are encouraged to visit:

http://www.elsevier.com/copyright

Author's personal copy

Journal of Crystal Growth 318 (2011) 1105–1108

Contents lists available at ScienceDirect

Journal of Crystal Growth

journal homepage: www.elsevier.com/locate/jcrysgro

Bi catalyzed VLS growth of PbTe (0 0 1) nanowires

V.V. Volobuev [a,*], A.N. Stetsenko [a], P.V. Mateychenko [b], E.N. Zubarev [a], T. Samburskaya [a], P. Dziawa [c], A. Reszka [c], T. Story [c], A.Yu. Sipatov [a]

[a] National Technical University "Kharkiv Polytechnical Institute", 61002, 21 Frunze Street, Kharkiv, Ukraine
[b] State Scientific Institution "Institute for Single Crystals", NAS of Ukraine, 61001, 60 Lenin Avenue, Kharkiv, Ukraine
[c] Institute of Physics PAS, Al. Lotnikow32/46, 02-668 Warsaw, Poland

ARTICLE INFO

Available online 2 December 2010

Keywords:
A1. Nanostructures
A1. Nanowires
A3. Molecular beam epitaxy
A3. Vapor–liquid–solid growth
B2. Semiconducting lead compounds

ABSTRACT

PbTe (0 0 1) nanowires have been synthesized by thermal evaporation in a high vacuum using vapor–liquid–solid growth mechanism with Bi catalyst on KCl (0 0 1) substrate. Transmission and scanning electron microscopy as well as X-ray diffraction technique were employed in order to inspect nanowire structure. Having rock salt (NaCl) structure, the nanowires uniform in diameter grew along [0 0 1] axis and were perpendicular to the substrate plane. The cross-section of PbTe nanowires was found to be rectangular in shape and nanowire walls turned out to be faceted by {1 0 0} plains that are the most energetically favorable type of planes for NaCl type of structure. Mean nanowire diameter was found to be 50–200 nm depending on size of Bi catalyst droplets. The half-width of (0 0 2) maximum on X-ray rocking curve was found of the order of 0.3–0.5°, no worse than typical value obtained for KCl substrate. No tapering and other defects like twins were observed.

© 2010 Elsevier B.V. All rights reserved.

1. Introduction

Nowadays attention of researchers is attracted by semiconductor nanowires (NW) due to their prominent physical properties and great potential for industrial applications [1]. Particularly, NWs made of IV–VI materials, and especially of PbTe, are perspective for thermoelectrics [2,3], infra-red lasers and detectors [4,5] as well as for multi-exciton generation in enhanced surface area solar cells [6,7].

Various techniques are utilized at present to obtain semiconducting NWs [1]. One of the most perspective and widely used is vapor–liquid–solid (VLS) process [8], where evaporated material is incoming onto liquid droplet surface of catalyst material and then precipitates from supersaturated liquid solution on liquid–solid interface, thereby making NW to grow under a droplet. A catalyst material usually is chosen to have limited solubility with NW material in liquid and solid state. Because of making low eutectic point with many semiconductors gold is widely used as catalyst. Despite of many advantages of Au in producing oriented, size-selected NWs, the main drawback is that gold can form deep level traps within the band gap of some semiconductors, deteriorating the electronic properties of NW materials [9]. Having eutectic type phase diagram with PbTe [10] and solubility less than 1 mol% [11], Bi can be considered for the suitable catalyst for PbTe NW growth. Moreover, n-type doping of PbTe with Bi and its telluride compounds is commonly used [12]. Also, bismuth has been already used as catalyst for VLS synthesis of PbSe NW networks [13].

In contrast to other methods, like widespread chemical vapor transport synthesis, molecular beam epitaxy (MBE) uses thermal evaporation of constituent materials and allows better control of growth process. Unfortunately, to our knowledge, there is only one work devoted to MBE growth of IV–VI NWs [14].

In this work, we present details of PbTe NW growth by simple method of thermal evaporation in a high vacuum using Bi as catalyst.

2. Experimental

Semiconductor PbTe NWs have been grown epitaxially via VLS mechanism on KCl (0 0 1) substrate at temperature of 375 °C under a high vacuum 10^{-7} Torr in home-built setup using bismuth particles as catalyst. For deposition of the materials simple thermal evaporation from tungsten boats was used. First, Bi seed layer was predeposited at room temperature. After that Bi particle arrays formed during annealing at NW growth temperature and then PbTe was deposited. For several samples additional flux of Bi was used during PbTe NW growth. Amount of deposited material and growth rates were controlled using a calibrated quartz balance resonator. The deposition rate of the NW components was 0.05–0.3 nm/s. Transmission (TEM) and scanning (SEM) electron microscopies as

* Correspondence to: Metal and Semiconductor Physics Department, National Technical University "Kharkiv Polytechnical Institute", 61002, 21 Frunze Street, Kharkiv, Ukraine. Tel.: +38 057 7510470; fax: +38 057 7076601.
E-mail address: volobuev@kpi.kharkov.ua (V.V. Volobuev).

0022-0248/$ - see front matter © 2010 Elsevier B.V. All rights reserved.
doi:10.1016/j.jcrysgro.2010.11.143

Author's personal copy

well as X-ray diffraction (XRD) technique were employed in order to inspect NW crystal structure. For electron microscopy studies NWs were covered with 20-nm-thick amorphous carbon layer in another home-built setup by dc magnetron sputtering method in Ar atmosphere. For TEM studies KCl substrate was dissolved in distilled water and after that samples were caught on TEM grids. Placing NW samples on grids folded in two enabled us to observe NWs with their axis perpendicular to electron beam (from side view) on the folded end of grids. XRD investigations were performed in $\theta-2\theta$ geometry using Cu-Kα_1 radiation.

3. Results and discussion

SEM images of PbTe NW initial growth stage is presented in perspective (axonometric) and plain (top) view in Fig. 1a and b. The effective thickness of predeposited Bi seed layer was 9 nm. The obtained nanocrystals were within 500–750 nm range in length and 150–300 nm in diameter. As one can see from Fig. 1a, there are droplets on tops of the nanocrystals as expected in VLS growth mechanism. Although growth directions of majority of nanocystals are perpendicular to the substrate, some of them lie with their axis parallel to the substrate. One side of the lying nanocrystal has semispherical shape indicating catalyst presence. Therefore not only vertical but also lateral growth of NWs is possible. The nanocrystals have rectangular cross-section and are faceted with {1 0 0} planes as it is seen from top view image (Fig. 1b). This set of planes is the lowest free-energy surfaces in IV–VI semiconductors [14–17], that makes {1 0 0} faceting energetically favorable for PbTe nanocrystal structures. The faceting has been observed previously for Ga–Au catalyzed (0 0 1) PbTe NWs on GaAs (1 1 1) B substrates prepared at the same substrate temperature [14]. In contrast to our case, PbTe NWs on GaAs had tapered shape and different substrate orientation therefore faceting with other sets of plains was also present. Electron diffraction (ED) pattern taken from the nanocrystals with their axis parallel to electron beam is shown in Fig. 1c. It is seen from the figure that obtained nanocrystals are monocrystalline, observed spots correspond to (0 0 1) orientation of fcc lattice. Interspace distances calculated from the pattern match well to PbTe. Thus the obtained nanocrystals grow along [0 0 1] axis and are perpendicular to the substrate plane.

Individual nanocrystals were investigated by TEM (see Fig. 2). In the bright field TEM image (Fig. 2a), striped PbTe nanocrystal body with a droplet of different contrast on nanocrystal top is seen. The PbTe nanocrystal is oriented with (1 1 0) plane perpendicular to electron beam as it is determined from selected area electron diffraction pattern (SAED) (Fig. 2c). Therefore two of the ribs of PbTe parallelepiped are faced to us and the observed stripes are thickness fringes. The dark field TEM image obtained from (0 0 −2) reflection of PbTe is shown in Fig. 2b. It is seen that the whole nanocrystal is in a reflecting position except a droplet on top which is concealed. The concealed droplet in Fig. 2b proves that the droplet is made of the material other than PbTe and can be an evidence of VLS growth mechanism.

Epitaxial growth and high quality of obtained PbTe nanocrystals was also confirmed by XRD (Fig. 3). The strong set of {0 0 1} PbTe maxima was observed proving (0 0 1) orientation of the nanocrystals. The full-width at half-maximum (FWHM) of (0 0 2) PbTe peak obtained from ω scan (see inset) is 0.46° which is no worse than FWHM typical values for KCl (0 0 1) substrate.

In order to decrease NW's diameter we have diminished size of catalyst droplet by decreasing effective thickness of Bi seed layer to 2 nm. As the result, nanocrystals with average diameter of 85 nm were obtained. TEM images of the nanocrystals are shown in Fig. 4. As it is seen from the side view TEM image (Fig. 4a), no droplets are present on the nanocrystal tops. The droplet disappearance is likely connected to

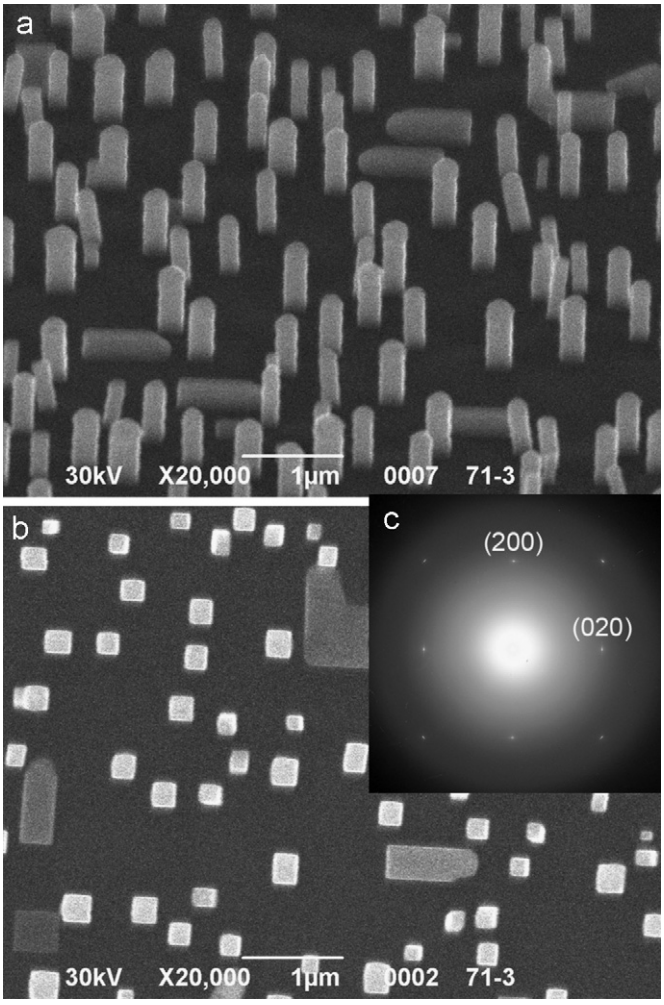

Fig. 1. Initial stage of PbTe NW growth: (a) SEM image side view, (b) SEM image top view, and (c) ED pattern (electron beam is parallel to nanowire axis), observed halo is from amorphous carbon layer. The effective thickness of predeposited Bi seed layer was 9 nm.

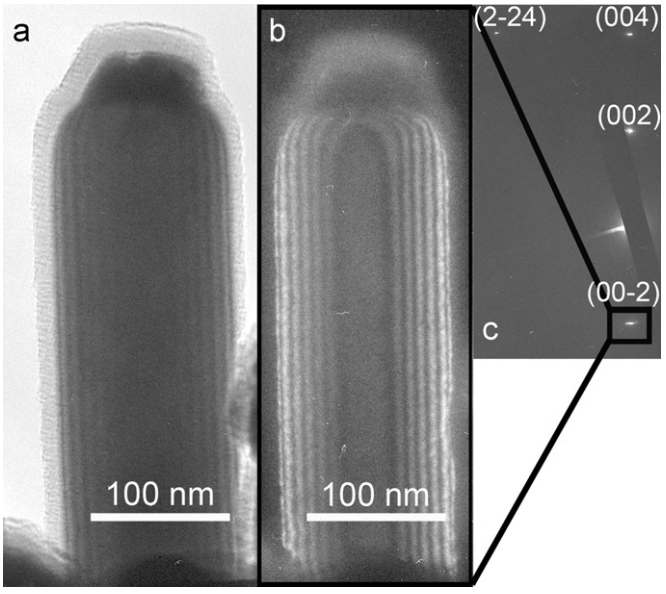

Fig. 2. TEM image of individual PbTe nanocrystal: (a) bright field, (b) dark field, and (c) SAED pattern. The observed amorphous shell is due to carbon cap layer presence.

Author's personal copy

its re-evaporation due to Gibbs–Thomson effect, when saturated vapor pressure of droplet material increases with decreasing of droplet diameter. The absence of droplets on top of nanocrystals results in axial growth stopping and coalescence of nanocrystals as it is seen from Fig. 4b. As the result, nanocrystal lateral growth prevails for further PbTe deposition and island thin film of complex form is emerged for deposited PbTe of larger amount.

Co-deposition of Bi and PbTe was performed in order to preserve droplets on nanocrystal tops. In our first experiments the deposition rates of Bi and PbTe were 0.3 and 0.05 nm/s, respectively. A side view of obtained condensates is presented in Fig. 5. Diameter of the crystals has been increased from hundreds nm to several μm in comparison to previously obtained samples. Large amount of bismuth had been deposited on a substrate during PbTe deposition makes catalyst nanodroplets expand in size strongly. Apparently that quantity of deposited PbTe was only enough to cover the bottom of Bi droplets. The large amount of deposited Bi was confirmed by XRD spectrum displayed in Fig. 6. The intensity of Bi maxima is even higher ones of PbTe. It should be noted that Bi lies epitaxially on PbTe with {0 1 2} sets of Bi plains parallel to {0 0 1} of PbTe. This can be easily understood as {0 1 2} plains of hexagonal Bi correspond to {0 0 1} Bi planes of pseudocubic lattice. The misfit in lattice parameter ($\Delta a/a$) between Bi and PbTe is less than 1% in this case.

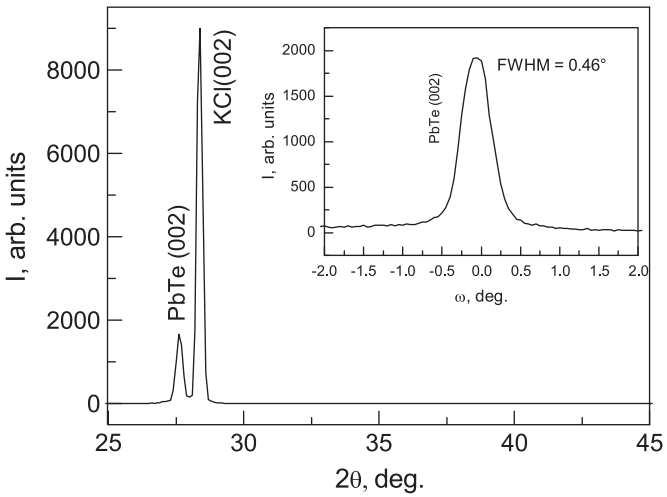

Fig. 3. X-ray diffraction pattern (θ–2θ scan) of PbTe NWs on (0 0 1) KCl substrate; ω scan is shown in the inset.

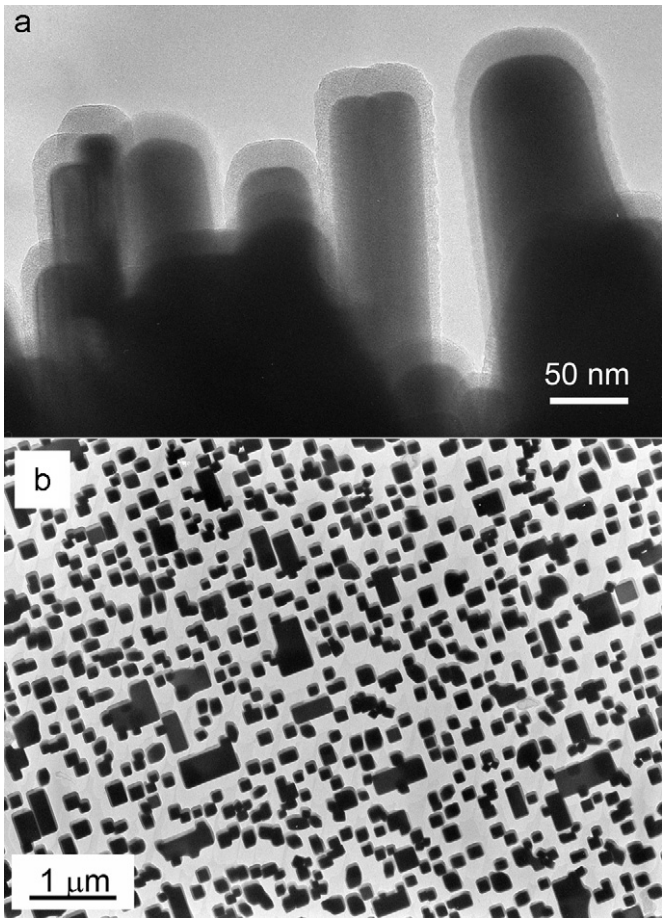

Fig. 4. TEM image of PbTe nanocrystals: (a) side view, and (b) top view. The effective thickness of predeposited Bi seed layer was 2 nm.

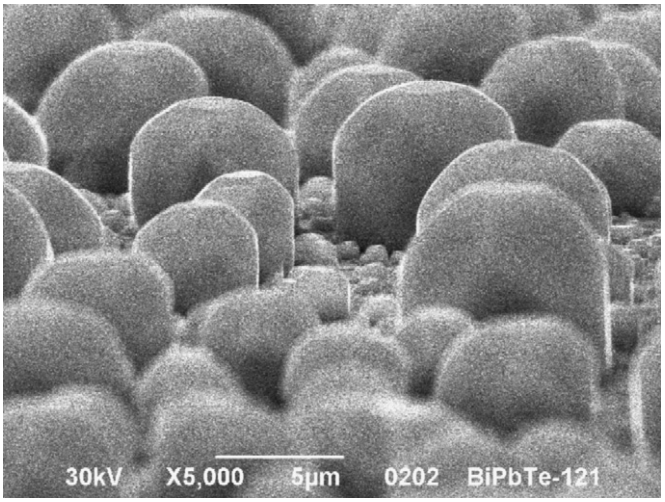

Fig. 5. SEM image of PbTe microcrystals obtained by co-deposition of Bi and PbTe. Bi and PbTe deposition rates were 0.3 and 0.05 nm/s, respectively.

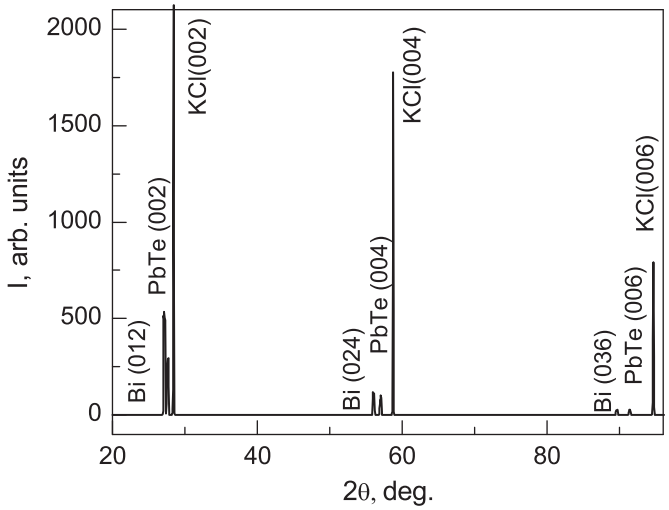

Fig. 6. X-ray diffraction pattern (θ–2θ scan) of PbTe microcrystals obtained by co-deposition of Bi and PbTe on (0 0 1) KCl substrate. Bi and PbTe deposition rates were 0.3 and 0.05 nm/s, respectively.

Author's personal copy

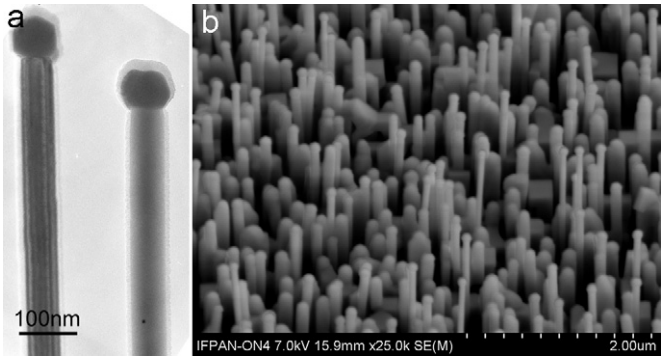

Fig. 7. TEM (a) and SEM (b) images of PbTe NWs obtained by co-deposition of Bi and PbTe. Deposition rate was 0.05 nm/s for both Bi and PbTe.

Further optimization of growth process led us to results presented in Fig. 7. For this sample, Bi was deposited in interrupted manner with the rate equal to PbTe deposition rate of 0.05 nm/s. After each 35 nm of pure PbTe deposition Bi evaporation source was switched on and 3 nm of Bi was co-deposited with PbTe. From the TEM image shown in Fig. 7a one can see that Bi catalyst is preserved on PbTe NW top. The NWs with diameter around 50 nm and length-to-diameter aspect ratio equal to 10 can be easily obtained using this technique. The side view SEM image of PbTe NW of the same sample is shown in Fig. 7a. The NWs of bigger diameters have smaller length and vice versa. It means that NWs with smaller diameters grow with higher rates.

In general, there are two basic mechanisms of evaporated atom delivery to NW tip. First mechanism is direct deposition from vapor on catalyst surface and the second is surface diffusion along NW sidewalls. In first case NWs with smaller diameters grow at smaller rates due to Gibbs–Thomson effect and growth rate can be even equal to zero for nanowires with diameter less than 100 nm [18]. In the second case the length of NW is inversely proportional to diameter [19] and NWs with smaller diameters grow faster. Thus, PbTe NWs growth is connected mainly to surface diffiusion.

4. Conclusions

Epitaxial arrays of high-crystal quality PbTe NWs have been obtained on (0 0 1) KCl substrate by Bi catalyzed vapor–liquid–solid mechanism. It has been shown that NWs uniform in diameter grew along [0 0 1] axis and were perpendicular to the substrate plane. The observed {1 0 0} faceting of PbTe NW sidewalls is connected to minimization of surface NW free energy. During growth of NWs with diameter less than 100 nm Bi catalyst vanishes due to Gibbs–Thomson effect. This problem is solved by co-deposition Bi and PbTe that allows preserving Bi droplet on NW top during NW growth. The NWs with smaller diameter grow faster than NWs with larger one that indicates NW building occurs by surface diffusion of adatoms along NW sidewalls.

Acknowledgements

Authors thank Prof. A.V. Tolmachev for support of SEM investigations and Dr. E.A. Bugaev for assistance in XRD experiments.

References

[1] M. Dresselhaus, Y. Lin, O. Rabin, M. Black, J. Kong, G. Dresselhaus, Nanowires, in: B. Bhusan (Ed.), Springer Handbook of Nanotechnology, Springer, Berlin, 2010, pp. 119–167.
[2] L. Hicks, M. Dresselhaus, Thermoelectric figure of merit of a one-dimensional conductor, Physical Review B 47 (1993) 16631–16634.
[3] Y. Lin, M. Dresselhaus, Thermoelectric properties of superlattice nanowires, Physical Review B 68 (2003) 75304.
[4] P. McCann, IV–VI semiconductors for mid-infrared optoelectronic devices, in: A. Krier (Ed.), Mid-infrared Semiconductor Optoelectronics, Springer, Berlin, 2006, pp. 237–264.
[5] G. Springholz, T. Schwarzl, W. Heiss, Mid-infrared vertical cavity surface emitting lasers based on the lead salt compounds, in: A. Krier (Ed.), Mid-infrared Semiconductor Optoelectronics, Springer, Berlin, 2006, pp. 265–301.
[6] A. Nozik, Multiple exciton generation in semiconductor quantum dots, Chemical Physics Letters 457 (2008) 3–11.
[7] M. Kelzenberg, S. Boettcher, J. Petykiewicz, D. Turner-Evans, M. Putnam, E. Warren, J. Spurgeon, R. Briggs, N. Lewis, H. Atwater, Enhanced absorption and carrier collection in Si wire arrays for photovoltaic applications, Nature Materials 9 (2010) 239–244.
[8] R. Wagner, W. Ellis, Vapor Liquid Solid Mechanism of Single Crystal Growth, Applied Physics Letters 4 (1964) 89–90.
[9] W. Bullis, Properties of gold in silicon, Solid-State Electronics 9 (1966) 143–168.
[10] R. O'Shea, J. Donovan, E. Peretti, The quasibinary system PbTe–Bi, Transactions of the Metallurgical Society of AIME 221 (1961) 1266–1267.
[11] N. Abrikosov, E. Skudnova, L. Poretskaya, T. Osipova, Investigation of the system of Bi–Pb–Te, Inorganic Material 5 (1969) 630–633.
[12] G. Springholz, Molecular beam epitaxy of IV–VI heterostructures and superlattices, in: D. Khokhlov (Ed.), Lead Chalcogenides: Physics and Applications, Taylor & Francis, New York, 2003, pp. 123–207.
[13] J. Zhu, H. Peng, C. Chan, K. Jarausch, X. Zhang, Y. Cui, Hyperbranched lead selenide nanowire networks, Nano Letters 7 (2007) 1095–1099.
[14] P. Dziawa, J. Sadowski, P. Dluzewski, E. Lusakowska, V. Domukhovski, B. Taliashvili, T. Wojciechowski, L. Baczewski, M. Bukala, M. Galicka, R. Buczko, P. Kacman, T. Story, Defect free PbTe nanowires grown by molecular beam epitaxy on GaAs (1 1 1) B substrates, Crystal Growth Design 10 (2010) 109–113.
[15] R. Egerton, Surface free energies of lead telluride, Surface Science 24 (1971) 647–650.
[16] R. Blachnik, P. Wallbrecht, Comments on: surface free energies of lead telluride by RF Egerton, Surface Science 33 (1972) 209–210.
[17] M. Bukala, M. Galicka, R. Buczko, P. Kacman, Stability of III–V and IV–VI nanowires—a theoretical study, Physica E: Low-dimensional Systems and Nanostructures 42 (2009) 795–798.
[18] E. Givargizov, Fundamental aspects of VLS growth, Journal of Crystal Growth 31 (1975) 20–30.
[19] D. Kim, U.G. Sele, M. Zacharias, Surface-diffusion induced growth of ZnO nanowires, Journal of Crystal Growth 311 (2009) 3216–3219.